A comparison of different tuning methods applied to speed control of an electrical driveline with flexible coupling

Ali Aramesh

Abstract—**A coupling distributes shocks and vibrations to the load, resulting in poor performance. In this study the flexibility of jaw and spider coupling is investigated by using two flexible couplings with different rigidity. Moreover, several tuning methods are applied to design a speed controller, resulting in different solutions accordingly. Each solution can be applied to a specific application based on its constraints and objectives. Criteria such as rising time, overshoot and settling time are used as the basis of comparison.**

Index Terms—**Flexible coupling, vibrations, electrical driveline, *PI*-control and speed control.**

I. INTRODUCTION

COUPLINGS, as one of essential parts of the machines, attach the driver to the driven piece of machinery. They are used in an electrical driveline to transmit the mechanical power directly from one shaft to another with constant velocity [1]. Furthermore, small couplings should be able to correct the shaft misalignment without causing excessive stress, resulting in improved performance of the driveline. Also, diverse couplings' responses to vibration, shock, temperature, misalignment, high velocity, space constraints, and ease of installation or removal will benefit users [2]. Flexible polyurethane spider couplings are commonly used in machines due to their ability to absorb shocks and vibrations [3]. Jaw couplings particularly are recommended for torque transmission in continuous-duty electric motor driven machinery, pumps and gearboxes [4]. However using such couplings result in resonances and instability in various operating speeds which ultimately leads to a lower mechanical and control motion performance. Moreover, couplings misalignment may result in overshoot, exceeding the steady-state value and other deteriorated dynamics [5]. The main types of misalignment including axial, angular and radial displacement decreases the transmissible torque and lifetime of the coupling [6].

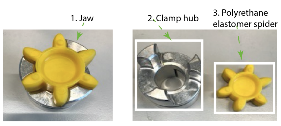

Fig. 1. Jaw and spider elastomer coupling

Burak and Dumanli [7] used optimal control theory to tune a controller for disturbance rejection and active vibration damping, and the results of their research revealed that it outperformed industry standard *PI*-control on a ball-screw drive in high-speed tracking studies. Yang and Wang [8] introduced a servo control system resonance frequency tracking strategy that uses velocity error and a band pass filter to track resonance and suppress vibration.

Flexible couplings prevent axial misalignment [9] between the drive and drive shafts along with transferring power from the motor to the shaft. Flexible connections other than the gear model are often used for low velocity and power. Yasufumi *et al.* [10], demonstrated control in a full-closed control system with anti-resonance vibration suppression. Understanding the inertia ratio and its effect on machine performance was addressed by Bryan Knight of Mitsubishi [11]. Schmidt and Rehm [12] have demonstrated a method for determining the resonance frequency of a dual inertia spring system by tuning an infinite impulse response notch filter with a FFT to decrease torsional oscillations in both the motor and load velocities. Bahn *et al.* [13] introduced a new algorithm for estimating the resonance frequency of adaptive notch filters used in servo systems that was considerably more effective in suppressing low- and high-frequency resonances. Misalignment between the shafts, torsional oscillations and late response to speed step response are some issues that leads to a low system performance, decrease of components' lifetime and instability of the system. Also, the use of different spider's rigidity lead to different results in terms of shocks and vibrations absorption, while a proper coupling prevents misalignment and accordingly decreases the overshoot [9]. Due to aforementioned challenges, this study seeks to apply different tuning methods including Auto-tune, Relay feedback and Bode-based to design a speed controller alongside Default method of SIEMENS. After that a speed step response is applied to analyze the behavior of the system. Criteria including rising time (t_{rise}), overshoot and settling time ($t_{settling}$) are considered as the basis of the comparison between the applied tuning methods. Furthermore two couplings with different rigidity are used in the setups to show their flexibility, as in flexible couplings, flexibility is provided by aligning sliding, or rolling [14]. Therefore applying different tuning methods alongside the use of jaw-spider coupling with polyurethane elastomer spider proposes an optimal solution for a wide range of applications, where high speed/torque or both are required. Therefore one can simply chooses a tuning method with respect to its objectives and constraints.

In the next section mathematical model of the system will be explained, in control method section, different tuning methods including Auto-tuning, Relay feedback and bode-based are elucidated. Afterward the experimental setups are explained in section IV, and the results are shown in section V. Finally, the conclusion of the research is discussed in section VI.

II. System modeling

A. Description of the mathematical model

A two-mass system can be used to model the mechanical system [15], in which the coupling is modeled by a parallel spring and damper, and the load and motor frictions by using two dampers. In the mathematical model a two mass spring damper system represents the system. Fig. 2 shows a coupled motor and a load.

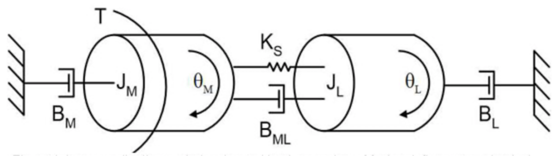

Fig. 2. A graphical model of a coupled motor and load [15]

TABLE I
PMSM and Load (induction motor) system parameters

Parameters	Description	Unit
J_M	Rotor inertia of the motor	$kg \cdot m^2$
J_L	Load inertia	$kg \cdot m^2$
K_s	Coupling elasticity	$kg \cdot m^2$
T	Applied torque	$N \cdot m$
B_{ML}	Viscous damping of the coupling	$N \cdot m \cdot s/rad$
B_M	Viscous damping between ground and rotor	$N \cdot m \cdot s/rad$
B_L	Viscous damping between ground and load	$N \cdot m \cdot s/rad$
E_M	Energy of motor(servo motor)	J
E_L	Energy of the load(induction motor)	J
$\dot{\theta}_M$	Motor speed of rotation	rad/s
$\dot{\theta}_L$	Load speed of rotation	rad/s
ω	Angular velocity	rad/s
f_{AR}	Anti-resonance frequency	Hz
f_{PM}	$\frac{1}{6}$ of f_{AR}	Hz
$\lvert G\rvert_f$	Corresponding amplitude of f_{PM}	dB

The equations of motion of the system illustrated in Fig. 2 are [1]:

$$\begin{aligned} T - B_M\dot{\theta}_M - B_{ML}(\dot{\theta}_M - \dot{\theta}_L) - K_s(\theta_M - \theta_L) = J_M\ddot{\theta}_M \\ - B_L\dot{\theta}_L + B_{ML}(\dot{\theta}_M - \dot{\theta}_L) + K_s(\theta_M - \theta_L) = J_L\ddot{\theta}_L \end{aligned} \quad (1)$$

Motion equations 1 are transferred to frequency domain through Laplace transform:

$$\begin{bmatrix} J_Ms^2 + (B_{ML} + B_M)s + K_s & -(B_{ML}s + K_s) \\ -(B_{ML}s + K_s) & J_Ls^2 + (B_{ML} + B_L)s + K_s \end{bmatrix} * \begin{bmatrix} \theta_M(s) \\ \theta_L(s) \end{bmatrix} = \begin{bmatrix} T(s) \\ 0 \end{bmatrix} \quad (2)$$

By rewriting 2 as a function of s, we obtain:

$$\left[J_Ms^2 + (B_{ML} + B_M)s + K_s\right] * \theta_M(s) = (B_{ML}s + K_s)\theta_L(s) + T(s) \quad (3)$$

$$\left[J_Ms^2 + (B_{ML} + B_M)s + K_s\right] * \theta_L(s) = (B_{ML}s + K_s)\theta_M(s) \quad (4)$$

Motor velocity at 500 $[rpm]$ decreases the viscous damping for both motor and load, therefore due to their small effect on resonance frequency, B_M and B_L parameters [15] can be set to zero, resulting in the following transfer functions:

$$\frac{\theta_M}{T}(s) = \frac{K[\frac{1}{\omega_{AR}^2}\cdot s^2 + \frac{2\zeta_{AR}}{\omega_{AR}}\cdot s + 1]}{s^2[\frac{1}{\omega_R^2}\cdot s^2 + \frac{2\zeta_R}{\omega_R}\cdot s + 1]} \quad (5)$$

and:

$$\frac{\theta_L}{T}(s) = \frac{K(\tau\cdot s + 1)}{s^2[\frac{1}{\omega_R^2}\cdot s^2 + \frac{2\zeta_R}{\omega_R}\cdot s + 1]} \quad (6)$$

Where:

$$K = \frac{1}{J_M + J_L}, \tau = \frac{B_{ML}}{K_s} \quad (7)$$

$$\zeta_{AR} = \frac{B_{ML}}{2\sqrt{K_sJ_L}}, \zeta_R = \frac{B_{ML}}{2\sqrt{\frac{K_sJ_MJ_L}{J_MJ_L}}} \quad (8)$$

The step response of second order system to step input should be under- or critically-damped, that's why the damping ratio was kept between zero and one to guarantee system stability, and it could be found from the data-sheet of the coupling spiders. Therefore by finding the poles of the system which is the zeros of the transfer function's denominator, the resonance and anti-frequency were obtained. This helps to decrease a 4th order transfer function to a second order.

III. Control methods

A. Description of different control tuning methods

To analyze the impact of the speed control parameters (K_p and T_i) on step response, several tuning methods were applied to design a *PI*-controller. Moreover *SINAMICS STARTER* has its default parameters for speed controller. In following, the process of each tuning method and Default tuning are explained.

In *SINAMICS STARTER* the control structure consists of cascaded loop including a position, speed and current control. In this study the focus is on the tuning speed controller. In cascaded loop, position, speed and current represented with a separate block diagram.

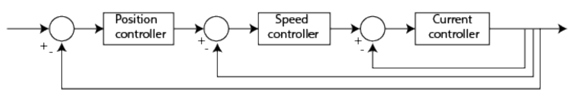

Fig. 3. Cascaded loop of the function generator of the *SINAMICS STARTER*

1) SIEMENS Default tuning: SINAMICS STARTER assigns 0.1418[Nms/rad] and 10[ms] to proportional(K_P) and integral(T_i) gains respectively to tune speed controller parameters. It should be added that *SINAMICS STARTER* is a power electronic software which was established by SIEMENS for commissioning drives and electrical drivelines.

2) Auto-tune method: The first two steps of the controller setting procedure are mechanical system measurement, followed by identification of the current control loop, and finally the computation of the speed controller setting. New speed controller parameters will be updated once the controller sequences have been completed.

3) Relay feedback tuning method: A required torque to drive the motor at $500[rpm]$ was considered, then a relay control was produced by setting the $T_i = 0$ and K_P big enough to saturate the controller. Moreover the protection of the system was guaranteed by setting the limit of the torque to $\pm 83\%$ of the steady-state torque. By doing so, a smooth change of the speed of the system was produced which is the output of the system. The tuning parameters for relay feedback

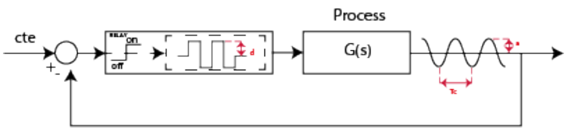

Fig. 4. The interaction between relay and process in Relay feedback tuning method

method were obtained by formulas tabulated in table II. In this

TABLE II
Speed controller parameters in Relay feedback method

Speed controller	K_P	T_i	K_c
PI	$K_P = 0.45.K_c$	$T_i = 0.83.T_c$	$K_c = \frac{4d}{\pi a}$

method, a square wave is applied to the input, in which the torque's amplitude and frequency is kept constant. The first harmonic is featured in the resulting output signal. A square wave is applied at the input as a relay to keep the torque at a constant amplitude and frequency. The steady-state torque of 0.26 $[N{\cdot}m]$ is obtained by running the motor at a speed of 500 $[rpm]$. The values of the upper and lower limits are derived using equation (9).

$$T_{upper/lower} = 0.26 \pm (0.83 * 0.26) \qquad (9)$$

Torque set point and speed are the input and output parameters of relay feedback, respectively.

In order to generate an input torque pulse the values of 10000 $[N{\cdot}m{\cdot}s/rad]$ and 0 $[ms]$ were assigned to K_p and T_i respectively.

4) Bode-based tuning method: Bode plot illustrates the characteristics of the system for different frequencies, such that resonance (f_R) and Anti-Resonance (f_{AR}) frequency of the system depends on the stiffness and damping ratio of the spring and damper respectively. From bode plot f_{AR} was read and divided by six to obtain crossover frequency. The corresponding amplitude was read and latter frequency and amplitude were lead to new K_P and T_i by using formulas tabulated in tableIII.

IV. Experimental S120 SINAMICS setups

A. Setup description

Each experimental setup was made up of several parts, including S120 SINAMICS drives, induction motor and PMSM

TABLE III
Speed controller parameters in Bode-based method

Speed controller	K_P	T_i
PI	$K_P = 10^{\frac{-1.25-\lvert G\rvert_f}{20}}$	$T_i = \frac{1.73}{2*\pi*f_{PM}}$

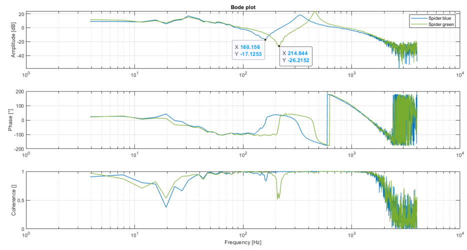

Fig. 5. Bode plot of the system for blue and green spider, input and output are current set point torque generating(r1650) and actual speed smoothed(r63)

motor, all of which were mounted on a mobile frame. The book-size control unit, line-, and motor modules were all included in the S120 SINAMICS servo drive package. A PMSM and an induction motor were coupled with a flexible coupling. The Permanent magnet synchronous technology was chosen as the motor, due to its encoder connected to the control unit. PMSMs are simple to operate and can precisely monitor the rotor position, according to [16].

B. Dynamics of the setup with flexible coupling

In this study, coupling is a key component that absorbs shocks and vibrations created by the motor, as well as the alignment of the motor and load. The results varied, depending on the rigidity of the polyurethane spider utilized in the coupling. Fig. 7 shows two polyurethane spider with different stiffness that were utilized in the couplings.

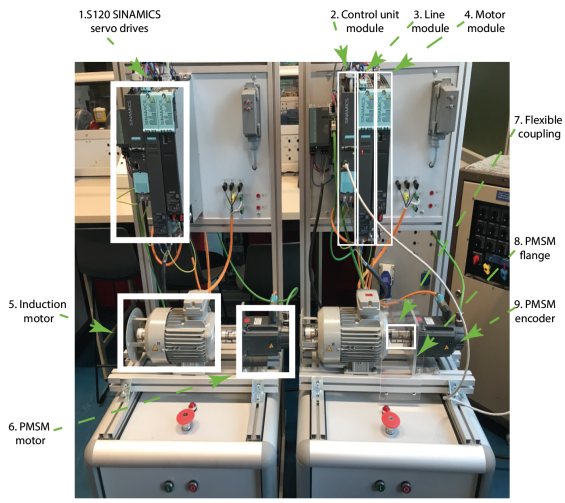

Fig. 6. The setups with different coupling spiders' rigidity

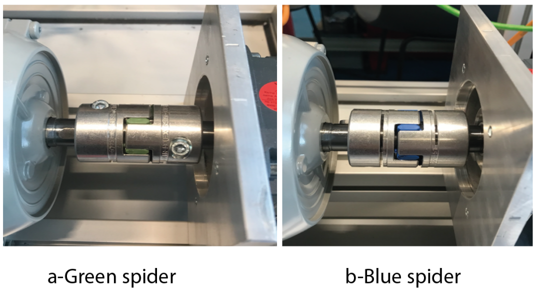

Fig. 7. Two different spiders with different rigidity used in the setups

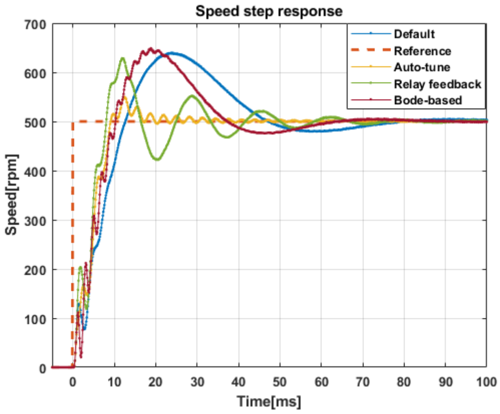

Fig. 8. Speed step response of different tuning methods for blue spider, input: Actual speed smoothed(r63) and output: Speed set point before the set point filter(r60)

V. Results and discussion

A. Speed step response analysis

Different tuning methods including Auto-tune, Relay feedback and Bode-based were carried out to design a *PI*-controller which were evaluated by a speed step response. The criteria that were considered as the basis of the comparison included rising time, overshoot and settling time. Experiments were performed on two types of flexible coupling to confirm its flexibility associated with aforementioned tuning methods.

The speed step response of different tuning methods were performed to see which tuning method has better performance regarding different criteria.

Figs. 8 and 9 shows the speed step response for blue and green spiders respectively. Despite of being easy to implement, obtained results for Bode-based results weren't better than Auto-tune and Relay feedback.

B. Experimental measurements

The measurement results tabulated in table V and VI shows a lower overshoot for blue spider, while rising- and settling time were obtained bigger in Relay feedback tuning method.

A quantitative comparison in tables VII and VIII [17] showed Auto-tune has the best performance in compare with other methods, although rise time is longer than Relay feedback method.

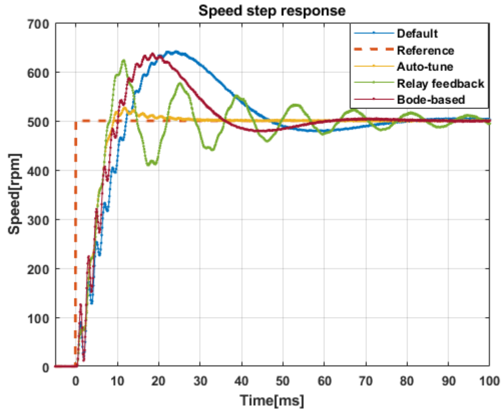

Fig. 9. Speed step response to different tuning methods for green spider, input: Actual speed smoothed(r63) and output: Speed set point before the set point filter(r60)

TABLE IV
Speed controller parameters for both experimental setups

Method	K_P		T_i	
	Blue	Green	Blue	Green
Default	0.1418	0.1418	10	10
Auto-tune	0.5989	0.599	13.35	12.31
Relay feedback	0.2649	0.313	1.243	1.142
Bode-based	0.1895	0.1857	10.316	7.6895

TABLE V
The results of measurements with blue spider

Method	T_{rise}	Overshoot	$T_{settling}$
Default	10.2232	27.8992	70.5176
Auto-tune	7.5967	9.9548	25.3090
Relay feedback	6.7814	25.7019	55.8084
Bode-based	8.0863	18.4692	36.3055

TABLE VI
The results of measurements with green spider

Method	T_{rise}	Overshoot	$T_{settling}$
Default	9.5851	28.2654	70.7251
Auto-tune	6.6041	5.2856	18.6762
Relay feedback	6.3520	24.6033	95.6521
Bode-based	7.7165	27.3498	53.9334

TABLE VII
Performance of different control tuning methods for blue spider(1: the best, 4: the worst)

Method	T_{rise}	Overshoot	$T_{settling}$
Default	4	3	4
Auto-tune	2	1	1
Relay feedback	1	2	2
Bode-based	3	4	3

TABLE VIII
Performance of different control tuning methods for green spider(1: the best, 4: the worst)

Method	T_{rise}	Overshoot	$T_{settling}$
Default	4	4	2
Auto-tune	2	1	1
Relay feedback	1	2	4
Bode-based	3	3	3

VI. Conclusion

In this study several tuning methods including Auto-tune, Relay feedback and Bode-based were applied to design a *PI*-controller to control the speed of the system, which was equipped with flexible coupling.

Among the carried out methods Auto-tune was effective against high overshoot, while rising time wasn't better than Relay feedback. Although Bode-based was simple to implement, the results for none of the spiders were better than Auto-tune and Relay feedback. Auto-tune had the best performance when all factors were given equal weight, followed by Relay feedback, Bode-based, and Default. So as, the non-linear transfer function causes a limitation between damping ratio and frequency from mathematical point of view, this issue could be overcome as the future perspective. Indeed with some optimisation techniques resonance and anti-resonance frequencies could be obtained, which should be the ones that experimental model produces.

Acknowledgment

The authors would like to thank the motion-control team of Electromechanical department of University of Antwerp for their valuable remarks during this work and providing the hardware components of the setups.

References

1 Moscrop, J., Cook, C., and Naghdy, F., "An analysis of motor/load inertia mismatch in machine tool servo systems," *IFAC Proceedings Volumes*, vol. 33, no. 26, pp. 229–234, 2000, iFAC Conference on Mechatronic Systems, Darmstadt, Germany, 18-20 September 2000. [Online]. Available: https://www.sciencedirect.com/science/article/pii/S1474667017391498

2 McCullough, M., "Understanding spiders and their role in jaw couplings," *World Pumps*, vol. 2000, no. 405, pp. 22–25, 2000. [Online]. Available: https://www.sciencedirect.com/science/article/pii/S0262176200800619

3 Johnson, C., "An introduction to flexible couplings," *World Pumps*, vol. 1996, no. 363, pp. 38–43, 1996. [Online]. Available: https://www.sciencedirect.com/science/article/pii/S0262176299810013

4 "Elastic jaw couplings created with low up-keep," *World Pumps*, vol. 2017, no. 10, p. 13, 2017. [Online]. Available: https://www.sciencedirect.com/science/article/pii/S0262176219301427

5 Verucchi, C., Bossio, J., Bossio, G., and Acosta, G., "Misalignment detection in induction motors with flexible coupling by means of estimated torque analysis and mcsa," *Mechanical Systems and Signal Processing*, vol. 80, pp. 570–581, 2016. [Online]. Available: https://www.sciencedirect.com/science/article/pii/S0888327016300747

6 Sawalhi, N., Ganeriwala, S., and Tth, M., "Parallel misalignment modeling and coupling bending stiffness measurement of a rotor-bearing system," *Applied Acoustics*, vol. 144, pp. 124–141, 2019, special Issue on ICTD-CMMNO'2016 (ICTD : International Congress on Technical Diagnostics). [Online]. Available: https://www.sciencedirect.com/science/article/pii/S0003682X17301068

7 Sencer, B. and Dumanli, A., "Optimal control of flexible drives with load side feedback," *CIRP Annals*, vol. 66, no. 1, pp. 357–360, 2017. [Online]. Available: https://www.sciencedirect.com/science/article/pii/S0007850617300495

8 Yang, S.-M. and Wang, S.-C., "Detection of resonance frequency in motion control systems," in *2013 IEEE Energy Conversion Congress and Exposition*, 2013, pp. 3757–3761.

9 Iurritegui, A., Gonzalez-Perez, I., Arana, A., Larraaga, J., and Ulacia, I., "Computerized generation and tooth contact analysis of spherical gear couplings for high misalignment applications," *Mechanism and Machine Theory*, vol. 164, p. 104408, 2021. [Online]. Available: https://www.sciencedirect.com/science/article/pii/S0094114X2100166X

10 Yoshiura, Y., Asai, Y., and Kaku, Y., "Anti-resonance vibration suppression control in full-closed control system," *IEEJ Journal of Industry Applications*, vol. 9, no. 3, pp. 311–317, 2020.

11 Knight, B., "Understanding inertia ratio and its effect on machine performance," in *MITSUBISHI ELECTRIC, changes for the better*, 2015.

12 Schmidt, P. and Rehm, T., "Notch filter tuning for resonant frequency reduction in dual inertia systems," in *Conference Record of the 1999 IEEE Industry Applications Conference. Thirty-Forth IAS Annual Meeting (Cat. No.99CH36370)*, vol. 3, 1999, pp. 1730–1734 vol.3.

13 Bahn, W., Kim, T.-I., Lee, S.-H., and Cho, D.-I. ., "Resonant frequency estimation for adaptive notch filters in industrial servo systems," *Mechatronics*, vol. 41, pp. 45–57, 2017. [Online]. Available: https://www.sciencedirect.com/science/article/pii/S0957415816301441

14 Boyce, M. P., "18 - couplings and alignment," in *Gas Turbine Engineering Handbook (Fourth Edition)*, fourth edition ed., Boyce, M. P., Ed. Oxford: Butterworth-Heinemann, 2012, pp. 693–719. [Online]. Available: https://www.sciencedirect.com/science/article/pii/B9780123838421000184

15 Lewotsky, K., "Understanding the mysteries of inertia mismatch," 2015, lUnderstanding the Mysteries of Inertia Mismatch. [Online]. Available: https://www.automate.org/industry-insights/understanding-the-mysteries-of-inertia-mismatch

16 Li, Y.-F. and Wikander, J., "Model reference discrete-time sliding mode control of linear motor precision servo systems," *Mechatronics*, vol. 14, no. 7, pp. 835–851, 2004. [Online]. Available: https://www.sciencedirect.com/science/article/pii/S0957415804000340

17 Derammelaere, S., Haemers, M., De Viaene, J., Verbelen, F., and Stockman, K., "A quantitative comparison between bldc, pmsm, brushed dc and stepping motor technologies," in *2016 19th International Conference on Electrical Machines and Systems (ICEMS)*, 2016, pp. 1–5.

Ali Aramesh Was born in Tehran, Iran, 1986. He received his BS.c degree in Electrical engineering from Azad University, central Tehran branch(iauctb). After that he started working as distributed control system(DCS) and relay expert in METANIR Co. in Iran. Currently he is doing his MS.c in joint master's degree in sustainable automotive engineering, a European's program with a collaboration with University of Antwerpen, Loughborough University, Deusto University and University of Bordeaux. His research interests include the control systems, machine learning, optimisation and vehicle dynamics.